Materials Research. 2018; 21(5): e20170864.
DOI: http://dx.doi.org/10.1590/1980-5373-MR-2017-0864

An Experimental Study of the Solidification Thermal Parameters Influence upon Microstructure and Mechanical Properties of Al-Si-Cu Alloys

***Mauricio Silva Nascimento*[a]*, *Antônio Tadeu Rogério Franco*[a], *Carlos Frajuca*[a], *Francisco Yastami Nakamoto*[a], *Givanildo Alves dos Santos*[a], *Antônio Augusto Couto*[b,c]**

[a]*Instituto Federal de Educação, Ciência e Tecnologia de São Paulo - IFSP, São Paulo, SP, Brasil*
[b]*Instituto de Pesquisas Energéticas e Nucleares - IPEN, São Paulo, SP, Brasil*
[c]*Universidade Presbiteriana Mackenzie, São Paulo, SP, Brasil*

Received: September 26, 2017; Revised: May 05, 2018; Accepted: May 16, 2018

Metals solidification involves the transformation of the molten metal back into the solid state. Solidification structures impact heavily on the final product's characteristics. The microstructure effects on metallic alloys properties have been highlighted in various studies and particularly the dendrite arm spacing influence upon the mechanical properties such as tensile strength has been reported. In the present investigation, Al-10wt%Si-2wt%Cu and Al-10wt%Si-5wt%Cu alloys were directionally solidified upward under transient heat flow conditions. The experimental results include solidification thermal parameters such as tip growth rate and cooling rate, optical microscopy, volume fraction of the eutectic mixture, primary dendritic arm spacing and ultimate tensile strength. Experimental growth laws of primary dendrite arm spacing as a function of the solidification thermal parameters are proposed. The Hall-Petch mathematical expressions were used to correlate the ultimate tensile strength as a function of the primary dendritic arm spacing. It was found that the alloy with higher copper content had a more refined structure. More refined structures had higher ultimate tensile strength values.

Keywords: *solidification, microstructure, primary dendrite arm spacing, mechanical properties, Al-Si-Cu alloy.*

1. Introduction

The liquid transformation into a solid is probably the most important phase transformation in applications of science and engineering materials[1,2]. Currently a large part of the concepts and methods developed in support of solidification research, which is the main phenomenon that occurs during casting, can be applied on an industrial scale, allowing a visible improvement in the manufactured parts quality, making solidification studies a powerful tool for its economic potential[3]. The microstructure effects on metallic alloys properties has been highlighted in various studies and particularly, the grain size influence and dendrite arm spacing upon the mechanical properties has been reported[1,4]. There are a lack of studies about multicomponent alloys solidification in transitional arrangements on specific literature[5]. The ternary system (Aluminum, Silicon and Copper) has excellent properties as mechanical strength, low density as compared to ferrous alloys and good flowability. These properties make the system a good choice on automotive and aerospace industry, calling researchers attention[3,6]. Costa *et al*[7] investigated the influence of silicon on the microstructure comparing directional upward and horizontal solidification for the alloys Al-6wt%Cu-4wt%Si and Al-6wt%Cu, demonstrating that silicon alloying contributes to significant refinement of primary/secondary dendrite arm spacings. Araujo *et al*[8] investigated the interrelation between the secondary dendrite arm spacing and microhardness for Al-3wt%Cu, Al-3wt%Si and al-3wt%Cu-5.5wt%Si alloys in horizontal directional solidification. Vasconcelos *et al*[9] investigated the interconnection between microstructure and microhardness of horizontal directional solidification for Al-6wt%Cu-8wt%Si alloys. In addition to the primary dendritic arm spacing, the morphology of the eutectic mixture influences the mechanical properties. Yildirim *et al*[10] found that the addition of niobium to an iron aluminides modifies the eutectic mixture, so that the alloys exhibited higher compressive strength. After the heat-treated, alloys exhibited ultra-high compressive strength and highly enhanced compressive fracture strain. There were no significant changes in the volumetric fractions of the phases and in the primary dendritic arm spacing after the heat treatment, being the change of the mechanical properties related to the morphology of the eutectic mixture.

In the present investigation, Al-10wt%Si-2wt%Cu (cited as 2Cu alloy) and Al-10wt%Si-5wt%Cu (cited as 5Cu alloy) alloys were directionally solidified upward under transient heat flow conditions. The experimental results include tip growth rate (V_L) and cooling rate (T_R), primary dendritic arm spacing (PDAS) and ultimate tensile strength (σ_{UTS}). These alloys were chosen so that only the Cu content was different, in order to analyze their influence. Controlling the thermic solidification parameters such as V_L and T_R, it is possible to predict the conditions to obtain the microstructures with the desired properties[11,12,13].

* e-mail: mauricio.nascimento@ifsp.edu.br

2. Experimental Procedure

The experimental apparatus consists of a solidification furnace in cylindrical form (figure 1), with external steel casing and refractory bricks. Inside the oven there are an electrical resistors connected to a control panel and two support tubes. The inner one being made of stainless steel AISI 304 and the outer steel SAE 1020. Between these tubes there is a layer of refractory cement. An inner tube is responsible for directing the water jet to the inner surface of the plate, made of SAE 1020 steel. The thickness of the plate in the heat exchange region is 5 mm thick. In the upper surface, where the ingot is positioned, it was sanded with 1200 mesh sandpaper. The ingot was manufactured in stainless steel AISI 304 with internal diameter of 60 mm, external diameter of 76 mm and height of 160 mm. Type K thermocouples were positioned at distances, relative to the plate, of 4, 8, 12, 16, 35, 53 and 73 millimeters.

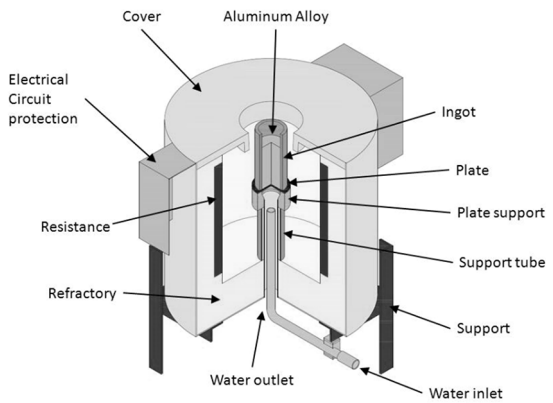

Figure 1. Schematic illustration of the upward unidirectional solidification furnace

The alloys were prepared in a graphite-clay crucible in a muffle-type electric furnace using commercially pure metals, which were analyzed by the X-ray spectrometry technique using a Spectro Spectromaxx Spectrometer (Table 1). Four casting leaks were performed for each of the alloys, all of them with a casting temperature of 700 ºC. The first ingot was used to analyze the solidification kinetics and preparation for micrographic analysis and the other three ingots were used to make test specimens for tensile tests. For each leak a sample was taken to check the composition of the prepared alloy. The analysis was performed by the X-ray spectrometry technique using a Bruker S2 Ranger Spectrometer (Table 2). After the pouring, the cooling started when the water jet was turned on at a flow rate of 21.6 L/min. All thermocouples were connected to a NI 9212 data acquisition module set and NI cDAQ 9171 chassis from National Instruments, which sent the collected data via USB cable to a computer, thereby allowing the collection of temperature data as a function of time at a rate of one die per second (Figure 2).

Figure 2. Upward unidirectional solidification furnace with control panel, data acquisition unit connected to thermocouples and computer to present and store experimental data.

The function P=f(t) was experimentally defined by the intersection of the straight line equivalent to *liquidus* temperature (T_L) of the alloy with the cooling curve of each thermocouple. By means of this intersection of the line the time of passage of the *liquidus* isotherm in that position of each thermocouple is determined. The derivative of the function P=f(t) allowed to obtain the respective experimental values for the displacement velocities of the *liquidus* isotherm (V_L), which corresponds to the liquid front passage through each thermocouple. The cooling rate (T_R) values for each position of the thermocouples were obtained experimentally from the intersections of the *liquidus* temperature line with the cooling curves of each thermocouple, through the result of the direct reading of the quotient of the temperatures before and after the temperature *liquidus* and the corresponding times ($\Delta T/\Delta t$).

Table 1. Chemical composition of the raw materials in weight %

Materials	Al	Si	Ca	Fe	Ti	Cu	Mg	Zn	NI	Cl	Other
Aluminum	99.8	0.071		0.095			0.001				0.033
Silicon	1.56	96.4	0.486	0.430	0.110		0.378			0.199	0.437
Copper	1.16	0.139	0.143			97.4		0.288	0.207	0.164	0.499

Table 2. Chemical composition of ingots in weight %

Alloy	Si	Cu	Fe	Other	Al
Al-10wt%Si-2wt%Cu	9.99	1.90	0.22	0.09	87.78
Al-10wt%Si-5wt%Cu	10.26	5.25	0.21	0.08	84.20

Transverse samples were taken from one of the solidified ingots for metallographic analysis at positions 5, 10, 20, 30, 40, 60 and 70 millimeters with respect to the cooling plate. These were embedded in bakelite, grinded and polished with diamond paste from 6 µm to 3 µm. The etchant used to reveal the microstructure was a 0.5% HF solution with a reaction time of approximately 22 seconds for the 2Cu alloy and 15 seconds for the 5Cu alloy. Optical microscopy was used to measure the PDAS for each selected position, and the triangle method was used[14]. At least 40 measurements were performed for each position, being performed only in the columnar region as a way to correlate this macrostructure with the thermal variables and tensile strength (Figure 3). The volume fraction of the phases observed in the metallographic examinations was calculated based on the systematic manual point count procedure described in ASTM E562 standards.

Figure 3. Representative schematic of the technique used to quantify the PDAS in a cross section.

The test specimens were made from three ingots, providing the tensile test of three test specimens for each position defined in Figure 4. The lower face of the ingot is the one that was in contact with theheat exchange plate.

The specimens were prepared according to ASTM E 8M standards with a diameter of 5 mm and a gage length of 25 mm. The equipment used for the test was a Kratos universal testing machine which has its own software for storing and displaying data. Figure 5 shows the sense of request of the specimen in relation to the microstructure obtained.

3. Results and Discussion

The *liquidus* temperature for the alloys under study were obtained in the Al-10%Si-XCu pseudo-binary diagram generated in the Thermocalc software version 2017a and is shown in Figure 6. It is observed that there is a difference of approximately 10 ºC between the two compositions.

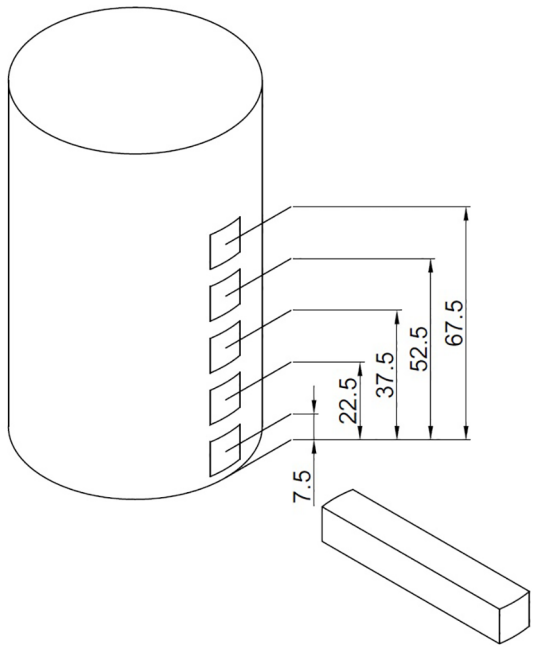

Figure 4. Location of test specimens for tensile testing (dimensions in millimeters).

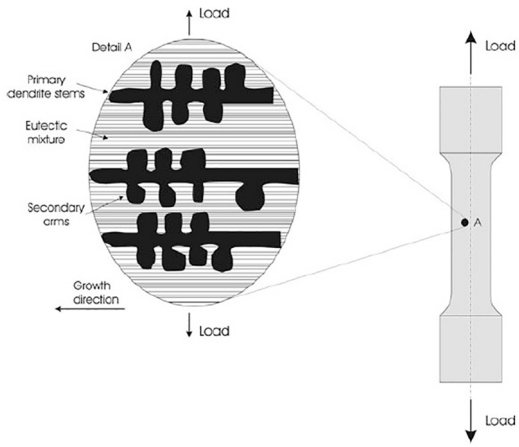

Figure 5. Illustrative drawing of the specimen as a function of the microstructure, direction of growth and direction of application of the tensile test[15].

Figure 7 shows the macrograph of an as-cast ingot evidencing the columnar structure obtained in the solidification. This structure is located from the heat exchange surface to a distance of 70 mm. In this position, for both alloys, there is a columnar/equiaxed transition (CET). Above this distance there is an equiaxed structure. This same procedure was performed for the other ingots, which were later cut for the preparation of the specimens.

The solidification thermal parameters obtained are shown in Figure 8. It can be seen that both V_L and T_R decreased as far from the surface, where heat is exchanged. The 5Cu alloy has lower value variation than 2Cu alloy from V_L.

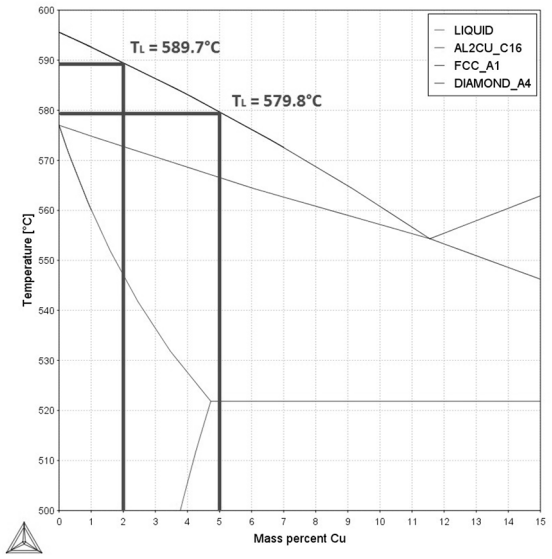

Figure 6. Pseudo-binary phase diagram Al-10% Si-XCu.

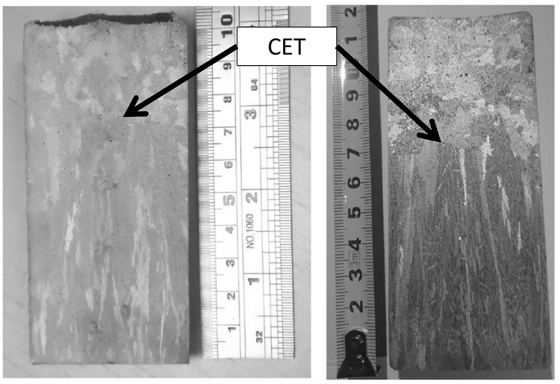

Figure 7. Macrostructures evidencing the columnar/equiaxed transition (CET): 2Cu alloy (left) and 5Cu alloy (right)

For T_R, the experimental points of the two alloys were very close (Figure 8 b). Thus, a single experimental equation was proposed for both alloys, evidencing that the percentage of Cu did not significantly change the T_R.

It is shown in Figure 9 the correlation between PDAS (λ_1) and distance from heat extraction surface (P). It is possible to see that 5Cu alloy has lower λ_1 values than 2Cu alloy, showing an influence of the copper on the microstructure. For both alloys, higher position values (P) tends to increase the λ_1 values.

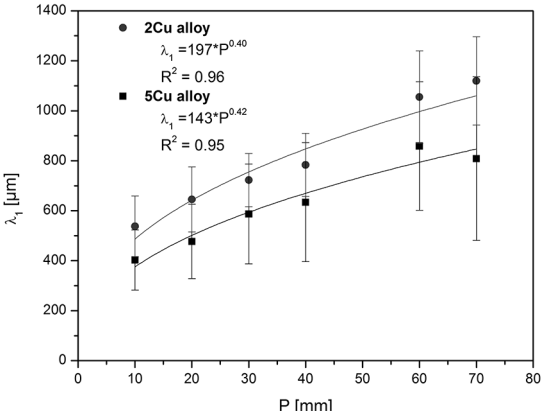

Figure 9. Primary dendrite arm spacing (PDAS). Correlation between PDAS (λ_1) value and heat-exchange surface (P).

The correlation among PDAS (λ_1), tip growth rate (V_L) and cooling rate (T_R) are shown in Figure 10. The value of the exponent is set to adjust the equation that relates λ_1 and T_R was -0.55 proposed by Bouchard and Kirkaldy[15] for binary alloys. Several authors[16,17,18,19] have used this value for ternary alloys obtaining satisfactory results. In Figure 10 a, λ_1 values tend to decrease with

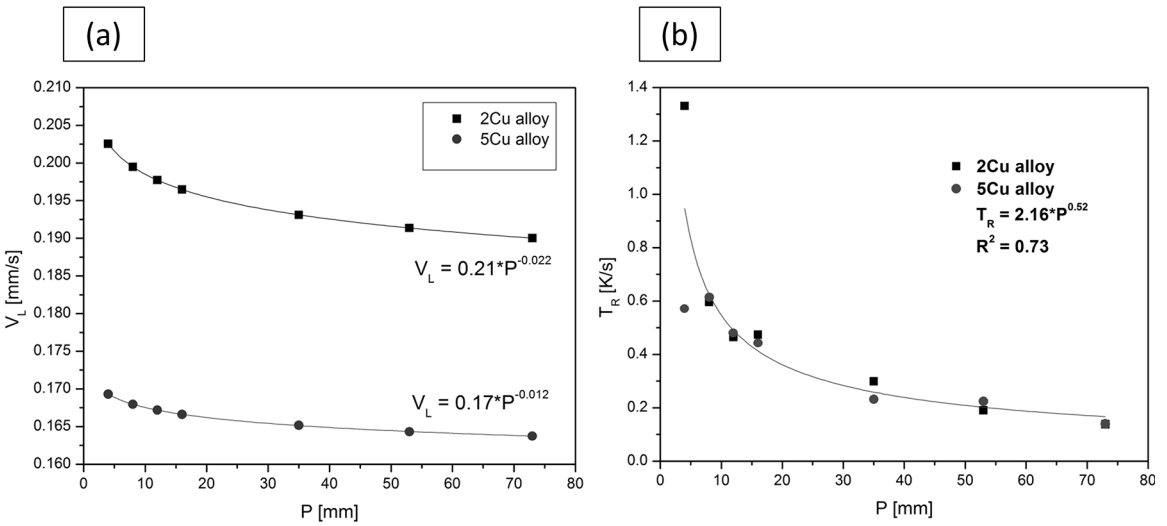

Figure 8. Solidification Thermal Parameters: (a) Correlation between Tip growth rate (V_L) and distance from heat extraction surface (P); (b) Correlation between cooling rate (T_R) and distance from heat extraction surface (P).

increasing T_R values. It is also observed that, for the 5Cu alloy, the values of T_R are lower than for the 2Cu alloy. In Figure 10 b, λ_1 values tend to decrease with increasing V_L values. The value of the exponent of the equation relating λ1 and V_L was different from -1,1 proposed by Bouchard and Kirkaldy[15] for binary alloys. Some authors[20, 21,22] have also found different values of exponent for V_L in ternary alloys. It is also observed that, for the 5Cu alloy, the values of V_L are lower than for the 2Cu alloy, demonstrating the influence of copper on the microstructure.

It is shown in Figure 11a, the correlation among ultimate tensile strength (σ_{UTS}) and the distance from heat-exchange surface. For higher position values the σ_{UTS} value tends to decrease. To correlate σ_{UTS} and λ_1, the Hall-Petch equation was used. The coefficients of the equations were defined by the least squares method. Several authors[19,23,24,25,26] used this methodology. These authors also primarily use PDAS, not the secondary dendritic arm spacing (SDAS), in columnar structures. As in this work only the columnar structure was analyzed it was decided to use λ_1. It is also possible to verify that the higher the copper rate, the higher the values of σ_{UTS}.

Figure 12 shows the transverse micrographs of the two alloys studied at positions 5, 20, 40 and 70 millimeters with respect to the heat extraction surface. It is observed that, for both alloys, the positions closest to the heat extraction surface have more refined structures. The 5Cu alloy presents lower λ_1 values than the 2Cu alloy in all positions, evidencing the influence of copper in the refinement of the microstructure. Because it was more refined, it was impossible to measure EDP at the 5 mm position for the 5Cu alloy. In this position we obtained an equiaxed structure, typical of the chill zone.

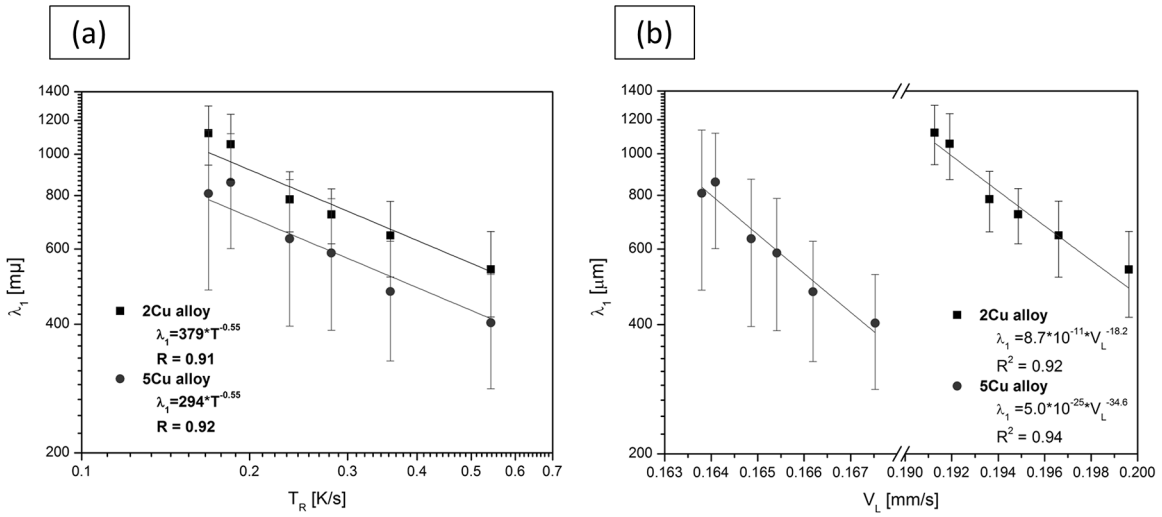

Figure 10. Primary dendrite arm spacing (PDAS). (a) Correlation between PDAS (λ_1) and cooling rate (T_R); (b) Correlation between PDAS (λ_1) and tip growth rate (V_L).

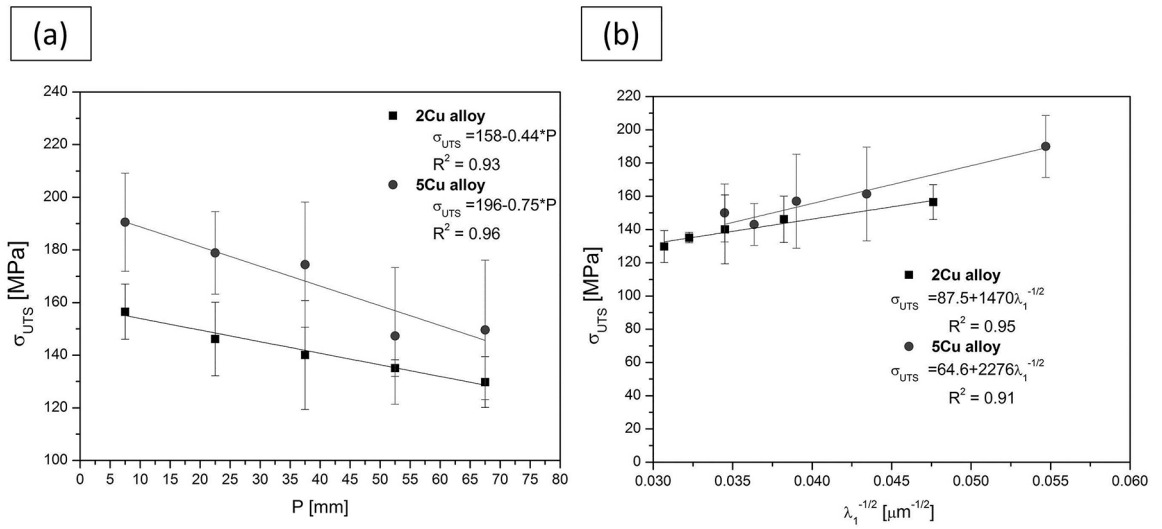

Figure 11. Ultimate tensile strength (σ_{UTS}). (a) Correlation between σ_{UTS} and surface distance; (b) Correlation between σ_{UTS} and PDAS (λ_1).

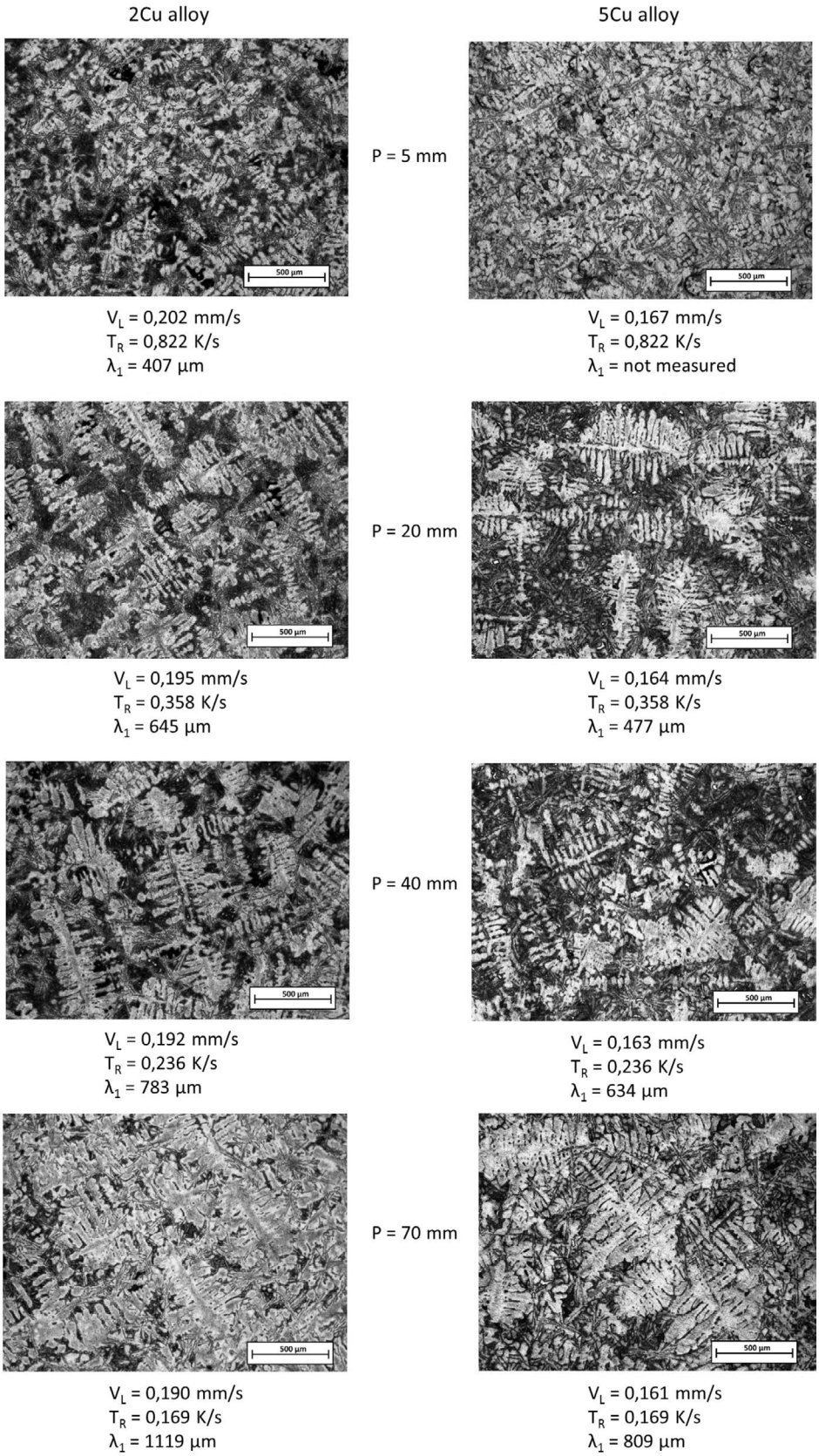

Figure 12. Micrograph: (left) 2Cu alloy; (right) 5Cu alloy.

The volumetric fraction of the eutectic mixture is presented in table 3. It is observed that the values of the volumetric fraction of the eutectic mixture decrease for larger distances of the surface of heat extraction, therefore for higher cooling rates, the greater the eutectic mixture fraction. This is in accordance with the literature[27] because higher cooling rates imply solidification out of balance, increasing the fraction of eutectic mixture.

Table 3. Volume fraction of the eutectic mixture

Position (mm)	2Cu Alloy	5Cu Alloy
5	0,590	0,509
20	0,598	0,552
40	0,552	0,576
70	0,473	0,473

4. Conclusions

In this experimental study on the influence of the solidification thermal parameters on the mechanical properties and microstructures of the 2Cu and 5Cu alloys, we can conclude:

1. The values of the solidification thermal parameters V_L and T_R decrease to positions furthest from the heat exchange surface. The V_L values are higher for the 2Cu alloy, evidencing the influence of the lower copper content. The values of T_R were very close to the two alloys, evidencing that the copper content does not influence this parameter.
2. PDAS values tend to decrease as the distance from the heat exchange surface increases. The 5Cu alloy presents lower values of PDAS than the 2Cu alloy for all positions, evidencing that a higher copper content contributes to the refinement of the microstructure.
3. When PDAS is correlated with the solidification parameters VL and TR, it is observed that, for higher values of VL and TR, the values of PDAS tend to decrease. The 5Cu alloy presents lower values in this correlation than the 2Cu alloy evidencing the influence of the higher copper content.
4. When the σ_{UTS} is correlated with the PDAS, it is observed that smaller values of PDAS present higher values of σ_{UTS}. This fact shows that more refined structures have higher σ_{UTS} values. The 5Cu alloy presents higher σ_{UTS} values than the 2Cu alloy in this correlation, evidencing the influence of a higher copper content.
5. The volumetric fraction values of the eutectic mixture increase for higher cooling rates for both alloys.

5. Acknowledgments

The authors acknowledge financial support provided by PROEQUIPAMENTOS 2014-CAPES (Higher Education Personnel Improvement Coordination).

6. References

1. Santos GA. *Tecnologia dos Materiais Metálicos: Propriedades, Estruturas e Processos de Obtenção*. São Paulo: Érica; 2015.
2. Groover MP. *Principles of Modern Manufacturing*. 5th ed. New York: Willey; 2013.
3. Ferreira AF, Castro JA, Ferreira LO. Predicting Secondary-Dendrite Arm Spacing of the Al-4.5wt%Cu Alloy During Unidirectional Solidification. *Materials Research*. 2017;20(1):68-75.
4. Osório WR, Goulart PR, Garcia A, Santos GA, Moura Neto C. Effect of dendritic arm spacing on mechanical properties and corrosion resistance of Al 9wt pct Si and Zn 27wt pct Al alloys. *Metallurgical and Materials Transactions A*. 2006;37(8):2525-2538.
5. Gomes LG. *Microestrutura dendrítica, macrossegregação e microporosidade na solidificação de ligas ternárias Al-Si-Cu*. [Thesis]. Campinas: State University of Campinas (UNICAMP); 2012.
6. Gomes CHU, Kikuchi RHL, Barros AS, Silva JNS, Silva MAPS, Moreira ALS, et al. On the Natural Convection in the Columnar to Equiaxed Transition in Directionally Solidified Aluminum-based Binary and Multicomponent Alloys. *Materials Research*. 2015;18(6):1362-1371.
7. Costa TA, Moreira AL, Moutinho DJ, Dias M, Ferreira IL, Spinelli JE, et al. Growth direction and Si alloying affecting directionally solidified structures of Al-Cu-Si alloys. *Materials Science and Technology*. 2015;31(9):1003-1112.
8. Araújo EC, Barros A, Kikuchi RH, Silva AP, Gonçalves FA, Moreira AL, Rocha OL. The Role of Si and Cu Alloying Elements on the Dendritic Growth and Microhardness in Horizontal Solidified Binary and Multicomponent Aluminium-Based Alloys. *Metallurgical and Materials Transactions A*. 2017;48(3):1163-1175.
9. Vasconcelos AJ, Kikuchi RH, Barros AS, Costa TA, Dias M, Moreira AL, et al. Interconnection between microstructure and microhardness of directionally solidified binary Al-6Wt%Cu and multicomponent Al-6wt%Cu-8wt%Si alloys. *Anais da Academia Brasileira de Ciências*. 2016;88(2):1099-1111.
10. Yildirim M, Akdeniz MV, Mekhrabov AO. Microstructural evolution and room-temperature mechanical properties of as-cast and heat-treated $Fe_{50}Al_{50-n}Nb_n$ alloys (n=1, 3, 5, 7, and 9 at%). *Materials Science & Engineering: A*. 2016;664:17-25.
11. Osório WR, Peixoto LC, Goulart PR, Garcia A. Electrochemical corrosion parameters of as-cast Al Fe alloys in a NaCl solution. *Corrosion Science*. 2010;52(9):2979-2993.
12. Song G, Bowles AL, St John DH. Corrosion resistance of aged die cast magnesium alloy AZ91D. *Materials Science and Engineering: A*. 2004;366(1):74-86.

13. Santos GA, Moura Neto C, Osório WR, Garcia A. Design of mechanical properties of a Zn27Al alloy based on microstructure dendritic array spacing. *Materials & Design*. 2007;28:2425-2430.

14. Gündüz M, Çardili E. Directional solidification of aluminium-copper alloys. *Materials Science and Engineering: A*. 2002;327(2):167-185.

15. Santos GA, Goulart PR, Couto AA, Garcia A. Primary Dendrite ARM Spacing Effects upon Mechanical Properties of an AL 3Wt%CU 1Wt%LI Alloy. In: Öchsner A, Holm Altenbach H, eds. *Properties and Characterization of Modern Materials. Advanced Structured Materials*. Volume 33. 1(st) ed. Singapore: Springer Singapore; 2017; p. 215-229.

16. Bouchard D, Kirkaldy JS. Prediction of dendrite arm spacings in unsteady and steady-state heat flow of unidirectionally solidified binary alloys. *Metallurgical and Materials Transactions B*. 1997;28(4):651-663.

17. Faria JD, Brito CC, Costa TAPS, Veríssimo NC, Santos WLR, Dias Filho JMS, et al. Influência na microestrutura e na microdureza decorrente da adição de 4%Ag na liga Al-4%Cu solidificada unidirecionalmente. *Matéria (Rio de Janeiro)*. 2015;20(4):992-1007.

18. Bertelli F, Brito C, Ferreira IL, Reichart G, Nguyen-Thi H, Mangelinck-Nöel N, et al. Cooling thermal parameters, microstructure, segregation and hardness in directionally solidified Al-Sn-(Si;Cu) alloys. *Materials & Design*. 2015;72:31-42.

19. Nascimento MS, Frajuca C, Nakamoto FY, Santos GA, Couto AA. Correlação entre variáveis térmicas de solidificação, microestrutura e resistência mecânica da liga Al-10%Si-2%Cu. *Matéria (Rio de Janeiro)*. 2017;22:e11774.

20. Carvalho RS. *A influência do cobre nas microestruturas e propriedades mecânicas de uma liga Al-2%Ni solidificadas com fluxo de calor unidirecional e transiente*. [Dissertation]. Brasília: University of Brasília (UnB); 2016.

21. Pinotti V, Braguin L, Reyes RV, Spinelli JE. Inter-relações entre microestrutura e parâmetros térmicos de solidificação de ligas monotéticas Al-(x)Bi-3%Cu. In: *Congresso Brasileiro de Engenharia e Ciência dos Materiais*; 2016 Nov 6-10; Natal, RN, Brazil.

22. Silva VCE, Spinelli JE, Bismarck LS. Microestrutura, Microdureza e Parâmetros Térmicos da liga de solda Sn-40%Bi-2%Ag. In: *Congresso Anual da ABM*; 2015 Aug 17-21; Rio de Janeiro, RJ, Brazil.

23. Goulart PG, Spinelli JE, Cheung N, Garcia A. The effects of cell spacing and distribution of intermetallic fibers on the mechanical properties of hypoeutectic Al-Fe alloys. *Materials Chemistry and Physics*. 2010;119(1-2):272-278.

24. Brito C, Vida T, Freitas E, Cheung N, Spinelli JE, Garcia A. Cellular/dendritic arrays and intermetallic phases affecting corrosion and mechanical resistances of an Al-Mg-Si alloy. *Journal of Alloys and Compounds*. 2016;673:220-230.

25. Bertelli F, Freitas ES, Cheung N, Arenas MA, Conde A, Damborenea J, et al. Microstructure, tensile properties and wear resistance correlations on directionally solidified Al-Sn-(Cu; Si) alloys. *Journal of Alloys and Compounds*. 2017;695:3621-3631.

26. Spinelli JE, Cheung N, Osorio WRR, Freitas ES, Garcia A. Correlação entre microestrutura, resistências mecânica e à corrosão da liga de soldagem livre de chumbo Sn-0,7%Cu. *Tecnologia em Metalurgia, Materiais e Mineração*. 2014;11(4):277-286.

27. Garcia A. *Solidificação: Fundamentos e Aplicações*. 2ª ed. Campinas: Editora Unicamp; 2007.